Slip distribution of the 1928 Chirpan and Plovdiv main shocks and earthquake triggering

Karakostas, V.[1], Papadimitriou, E.[1], Gospodinov, D.[2] and Ranguelov, B.[2]
1. Geophysics Department, Aristotle University of Thessaloniki, GR54124 Thessaloniki, Greece
2. Geophysical Institute, Bulgarian Academy of Sciences, Sofia, Bulgaria

Surface faulting and distribution of surface deformation caused by the Chirpan (M6.8) and Plovdiv (M7.0) earthquakes that occurred on 14 and 18 April 1928, respectively, were used with the scope to determine the distribution of slip and confirm the fault geometry. We assumed smooth fault geometry, based on previous studies, and a standard dislocation model. The faulting zone comprises several fault segments with different orientations and dips. For a structurally complex areas like our study area the best model may be to fix the strikes of the planes but allow the dip and rake to vary. Displacement on the different segments is also variable, showing large local concentrations. Fault geometry and slip distributions were used to calculate changes in static stress and interaction between the adjacent faults is discussed. Coulomb stress transferred by the Chirpan event has resulted in restressing of the adjacent fault segments, thus hastening the occurrence of Plovdiv event. Aftershock activity is also consistent with positive static stress changes.

Introduction

An earthquake of M6.8 occurred in Chirpan region of central Bulgaria on 14 April 1928 causing extensive damage in the nearby urban areas. This event was followed by a larger mainshock four days later (18 April 1928) that occurred to the southwest, in Plovdiv area (Fig. 1). Information on magnitudes and intensities of the two events is given by Christoskov (2000). Geodetic measurements performed in the area revealed the normal character of the associating faulting (Yankov, 1945). Numerous aftershocks were recorded during the following month, 14 of them with $M \geq 5.0$ (van Eck and Stoyanov, 1996). The largest of those was an M5.7 earthquake on 25 April near the village of Gulubovo, ~50km east of the first shock (Vanneste et al., 2006). Isoseismal of the three largest events of this seismic excitation are constructed by Shebalin (1974) and Papazachos et al. (1997).

During the 14 April earthquake two main parallel surface breaks formed, trending 100–110^{o}E with a distance between them equal to 15 km. Both were reported to have a throw of 0.3–0.4 m, down to the south and down to the north, respectively (Bonchev and Bakalov, 1928). The continuous south–dipping rupture had a 38–km length and an average 40 cm, reaching a maximum of 50 cm in the middle (DIPOZE, 1931). The 18 April earthquake generated a 53–km–long system of discontinuous breaks, trending 120–160^{o}E, with throws up to 1.5 m, and in one place even up to 3.5 m, down to the north.

The area under study is located in the Sub–Balkan graben (central Bulgaria), which defines the northern boundary of the Aegean extensional

system. This boundary is marked by the N–S to NNE–SSW extension present within central and northwest Bulgaria as confirmed by the overall kinematics shown by GPS (Kotzev et al., 2001). Most of the recent topography is of extensional origin, as suggested by Zagorchev (1992), Tzankov et al. (1996), and Burchfiel et al. (2000). Studies of earthquake focal mechanisms also indicate that active tectonism is dominated by north–south extension, with rare indications of strike–slip (Van Eck and Stoyanov, 1996). The east–west trending faults show only evidence for dip–slip movement and there is little or no field data to support strike–slip displacement on most of the faults. Some faults of north–eastern and north–western strike show evidence for strike–slip and others can be interpreted to have a strike–slip component (Burchfiel et al., 2000).

Kotzev et al. (2006) analyzed Global Positioning System (GPS) data acquired between 1996 and 2004 and fault plane solutions for four seismic zones to obtain the velocity and strain rate fields for western Bulgaria. Three fault plane solutions indicate NNE–striking faults (Georgiev, 1994) along which the 1928 earthquakes took place (Michailovic, 1933).

This study pursues to clarify the geometry and kinematics of the fault system in order to testing them with the observed surface deformation (Yankov, 1945). Finally, we use fault geometry and slip distributions to calculate changes in static stress, and we discuss the nature of interaction between the two events.

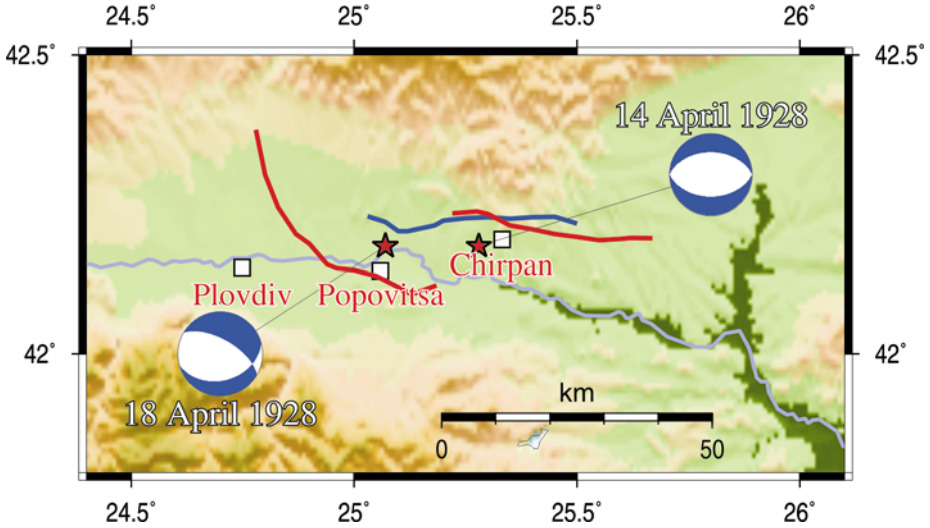

Fig. 1. *Relief map of the area of study. Surface ruptures of the Chirpan and Plovdiv earthquakes are shown by thick red lines (after S. Bonchev and Bakalov, 1928). Redetermined surface rupture of the Chirpan earthquake (G. Bonchev, 1931) is shown by thick blue line. The epicenters of the two strong events are depicted by red stars. Fault plane solutions are shown as equal–area lower–hemisphere projections. Locations of the nearby cities are shown by white squares and their names are written next by.*

Modeling Surface Displacements

We compare our modeled displacements with those obtained from geodetic measurements by Yankov (1945). We used the fault planes shown in Figure 1, which were derived from published fault plane solutions. Vanneste et al. (2006) suggest that only the north surface break is the direct expression at the surface of the fault that generated the 14 April earthquake, which is a long regional fault striking E–W and dipping to the south. Dimitrov et al. (2006) failed in determining the fault plane solution from the collected available data of P first arrivals while Jackson and McKenzie (1988) suggested a focal mechanism from surface ruptures (strike = 105^o, dip = 45^o, rake = $–90^o$). This latter solution is in agreement with a recently determined of a smaller magnitude event (09/09/1991, strike = 108^o, dip = 37^o, rake = $–99^o$) by Alexiev and Georgiev (2002). In our paper, we adopted a solution in good agreement with the latter two (strike = 95^o, dip = 45^o, rake = $–90^o$) and in accordance with the surface ruptures mapped by Bonchev and Bakalov (1928).

Fault plane solutions published for the Plovdiv event from Glavcheva (1984), VanEck and Stoyanov (1996), Dimitrov and Ruegg (1994) indicated a WNW–ESE oriented normal fault with a significant dextral component. The data used for the solution were only from remote stations, since there were no data from proximate stations, and most probably, this fact resulted in the solution of normal/strike–slip character (Alexiev and Georgiev, 1996). The more recent determination, based on newly collected data by Dimitrov et al. (2006), give a north–dipping fault plane in good agreement with the main surface rupture latter (strike = 300^o, dip = 67^o, rake = $–124^o$). The most suitable orientation of the fault plane related to Plovdiv event is that being in agreement with surface ruptures (strike = 300^o, dip = 62^o, rake = $–65^o$) and the orientation of the axis of maximum extension in the area (Kotzev et al. 2006), resulting to a left–lateral strike slip component added to the normal faulting (Fig. 2). The parameters of these fault planes are summarized in Table 1.

We assumed that surface deformation was caused by variable slip on several fault segments of the two causative faults embedded in an elastic half space (Okada, 1992). For the Chirpan fault, we considered three fault segment with different slip values on them, the maximum being on the western and upper fault patch. Considering a fault length of 38 km and width of 14 km, and aking a rigidity of 33·GPa and dislocations of 1.00 m, 0.30 m and 0.11 m for the three segments, respectively, we obtain a scalar moment (M_o=μSu) of $0.623 \cdot 10^{26}$ dyn·cm (Table 1). This corresponds to a moment magnitude of M_w6.5, in satisfactory agreement with the surface wave magnitude reported for this event (M_s6.8). For the Plovdiv fault, we considered sixteen fault patches with dislocation varying between some centimeters and 2.48 meters. If we consider a planer fault, its length equals to 47 km (53 km if we consider bends), which is used along with a fault width of 19 km to compute a scalar moment of $2.345 \cdot 10^{26}$ dyn·cm. This gives a moment magnitude of M_w6.9, which is much closer to the value reported for this event (M_s7.0).

Table 1. *Summary of fault parameters*

Date	Fault segment	Strike (°)	Dip (°)	Rake (°)	Length (km)	Width (km)	M_o (dyn·cm)
14 April	Chirpan	95	45	–90°	38	14	$0.623 \cdot 10^{26}$
18 April	Plovdiv	300	62	–65°	47	17	$2.345 \cdot 10^{26}$

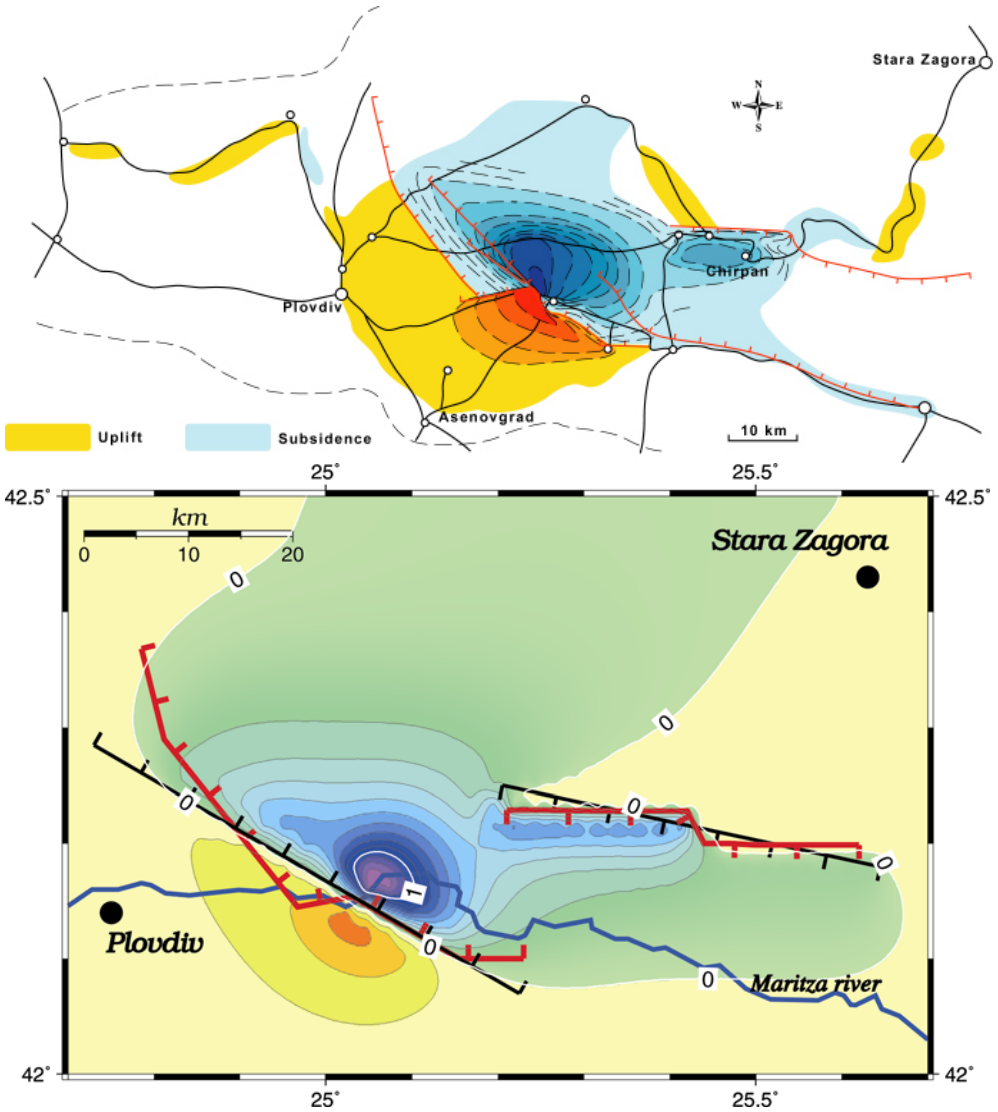

Fig. 2. *Horizontal displacement field on the surface of a homogeneous half–space due to Chirpan and Plovidv earthquakes. Contours denote the amplitude of displacement (in meters).*

Our synthetic displacements (Fig. 2, lower part) fit quite well those observed by Yankov (1945) as far as the shape and the magnitude concerns (Fig. 2, upper part). The abrupt alteration between uplift and subsidence around the middle of the Plovdiv fault cannot be predicted by the elastic model, which requires continuous displacements. This twisting of the isocontours is probably due to local landslides. Our slip model gives better

fit that the model of Dimitrov et al. (2006), who reproduced the displacement field using a homogeneous slip equal to 0.7 m on the Chirpan fault and ten fault patches for the Plovdiv fault with maximum slip equal to 2.6 m.

Coseismic deformation induced by the Chirpan earthquake on the Plovdiv fault

To assess the nature of any interaction between the two large events, we calculated static Coulomb failure stress change (ΔCFF) using the recovered slip distributions. Although the coseismic strain concentration on the Plovdiv fault adjacent to Chirpan rupture has been documented in a previous study (Papadimitriou et al., 2006), we examine the stress pattern here, since the geometry and slip distribution on the Chirpan is redefined in the present study in more detail. We used the formula of Okada (1992), assuming the fault system to be buried in a homogeneous half space with an apparent frictional coefficient of 0.4 (King et al., 1994). The shear modulus and Poisson's ratio are fixed as 33 GPa and 0.25, respectively. Using the information outlined in the previous section and Table 1, we modeled the ΔCFF in our study area. The stress field is calculated assuming an oblique normal faulting for the Plovdiv earthquake. Figure 3 shows the distribution of ΔCFF immediately after the Chirpan earthquake on a horizontal plane at a depth of 10 km.

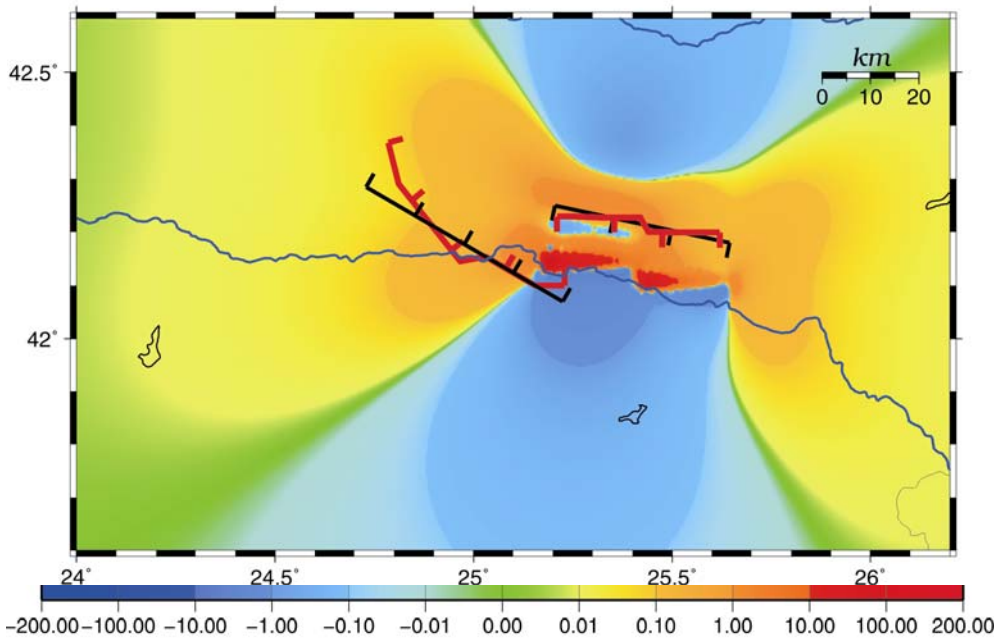

Fig. 3. *Coulomb static stress calculation at a depth of 10 km for the slip of the Chirpan earthquake computed for the faulting geometry of the Plovdiv earthquake, assuming normal faulting with a sinistral strike–slip component. Changes are denoted by the color scale at bottom (in bars). Red areas denote increase of the likelihood of slip on faults with the same geometry.*

The ΔCFF is positive where the Plovdiv fault is located, with positive static stress changes reaching up to 10 bars, as well as where the aftershock activity was concentrated. This elastic stress change may lead to earlier failure at the second rupture zone, a phenomenon known as *clock advance*. Reasenberg and Simpson (1992) and King et al. (1994) have suggested that static stress changes as low as 0.1 bar can induce aftershocks. The numerous aftershocks reported, as mentioned in a previous section, may well be explained by induced stress.

Discussion and conclusions

This study represents a step forward toward defining the slip distribution on faults of past earthquakes for which the relevant geodetic data are available. We tried to constrain the distribution of slip over the several fault patches in which the two main faults were divided. The compliant fault zone model that better explains the surface deformation successfully reveals that dip–slip is the dominant coseismic motion for the Chirpan earthquake, while the Plovdiv faulting encompasses strike–slip motion in addition to the dominant regional extension.

With better knowledge of the fault geometry and coseimic slip distribution for the Chirpan earthquake, stress changes were estimated in the study area. The fault zone near the hypocenter of the Plovdiv earthquake is loaded by slip associated with the Chirpan event. The Plovdiv earthquake did not occur immediately but the loading was sufficient to initiate the inevitable failure. Strong earthquakes are sometimes clustered in time, suggesting that fault failure on one fault may affect earthquake occurrence on another fault. The phenomenon of double strong event occurrence is quite common in the south Balkan area (see 1904, 1930, 1978 seismic sequences, more details in Papadimitriou et al., 2006). It may well be, then, that a recognizable pattern of stress and fault zone behavior will be the basis for anticipating the characteristics of future seismic excitations.

Acknowledgements. The stress tensors were calculated using the DIS3D code of S. Dunbar, which later improved by Erikson (1986) and the expressions of G. Converse. The GMT system (Wessel and Smith, 1998) was used to plot the figures. This study was supported by the bilateral research project between Greece and Bulgaria EPAN–M.4.3.6.1 and NZ–1209/02. Geophysics Department contribution 669.

References

Alexiev, G. and Georgiev, Tz., 1996. Geodynamic problems of the Kraishte–Sredna Gora morphostructural zone. *Problems of Geography*, *Bulg. Acad. Sci.*, 4, 131–140.

Alexiev, G. and Georgiev, Tz., 2002. Quaternary and recent geodynamic deformations of the territory of Bulgaria. *Problems of Geography, Bulg. Acad. Sci.*, 1–2, 30–48.

Bonchev, S. and Bakalov, P., 1928. Les treblements de terre dans la Bulgarie du sud les 14 et 18 avril 1928. *Rev. Vulg. Geol. Soc.*, 1(2), 51–63.

Burchfiel, C. B., Nakov, R., Tzankov, T. and Royden, L. H., 2000. Cenozoic extension in Bulgaria and northern Greece: the northern part of the Aegean extensional regime. *Geol. Soc. London, Spec. Publ.*, 173, 325–352.

Christoskov, L., 2000. Energy and source parameters of the strong Bulgarian earthquakes after 1900. *Rep. Geod., Warsaw Univ. of Technol., 3*(48), 15–20.

Dimitrov, D. and Ruegg, J.–C., 1994. The 1928 Bulgarian earthquakes: fault geometry from geodetic data and modeling, *1st International Symposium on Deformations in Turkey, Istanbul*, 921–932.

Dimitrov, D. S., Chabalier, J.–B., Ruegg, J.–C., Armijo, R., Meyer, B. and Botev, E., 2006. The 1928 Plovdiv sequence (Bulgaria): fault model constrained from geodetic data and surface breaks (*submitted*).

Direction for Support and Reconstruction of the area damaged by the 1928 Earthquakes (DIPOZE), 1931. *Report on the activities undertaken from April 25, 1928 until November 1, 1931* (in Bulgarian), State Press, Sofia, 421 pp.

Erikson, L., 1986. *User's manual for DIS3D: A three–dimensional dislocation program with applications to faulting in the Earth*. Masters Thesis, Stanford Univ., Stanford, Calif., 167 pp.

Georgiev, Tz., 1994. Seismotectonic characteristics of the dislocation line along the river valley of the Strjama, *Geophys. J. Bulg. Acad. Sci.*, XX, 50–56.

Glavcheva, R., 1984. Characteristic of the destructive earthquake of April 18, 1928 M=7.0) in Southern Bulgaria, *Geophys. J. Bulg. Acad. Sci.*, XVI, 38–44.

Jackson, J. A. and McKenzie, D. P., 1988. The relationship between plate motions and seismic tensors, and the rate of active deformation in the Mediterranean and Middle East. *Geophys. J. Intern.*, 93, 45–73.

King, G. C. P., Stein, R. S. and Lin, J., 1994. Static stress changes and the triggering of earthquakes. *Bull. Seism. Soc. Am.*, 84, 935–953.

Kotzev, V., Nakov, R., Burchfiel, B. C., King, R. and Reilinger, R., 2001. GPS study of active tectonics in Bulgaria: results from 1996 to 1998. *J. Geodynamics,* 31, 189–200.

Kotzev, V., Nakov, R., Georgiev, Tz., Burchfiel, B. C. and King, R. W., 2006. Crustal motion and strain accumulation in western Bulgaria. *Tectonophysics*, 413, 127–145.

Matova, M., Spiridonov, H., Rangelov, B. and Petrov, P., 1996. Major active faults in Bulgaria. *J. Earthq. Pred. Res.*, 5, 436–439.

Michailovic, J., 1933. La seismicite de la Bulgarie du Sud. *Monographies et travaux scientifiques, Serie B Institut Seismologique de l' Universite de Beograd, Beograd,* 46pp.

Okada, Y., 1992. Internal deformation due to shear and tensile faults in a half–space. *Bul. Seism. Soc. Am.*, 82, 1018–1040.

Papadimitriou, E., Karakostas, V., Tranos, M., Ramguelov, B and Gospodinov, D., 2006. Static stress changes associated with normal faulting earthquakes in south Balkan area (*submitted manuscript*).

Papazachos, B., Papazachou, C., 2002. *The earthquakes of Greece*. Ziti Publications, Thessaloniki, 317pp.

Papazachos, B. C., Papaioannou, Ch. A., Papazachos, C. B. and Savvaidis, A. S., 1997. Atlas of Isoseismal maps for strong shallow earthquakes in Greece and the surrounding area (426BC–1995). *Publ. Geophys. Lab., Univ. Thessal.*, 4, 194 pp.

Papazachos, B. C., Scordilis, E. M., Panagiotopoulos, D. G., Papazachos, C. B. and Karakaisis, G. F., 2004. Global relations between seismic fault parameters and moment magnitude of earthquakes. *10th Congr. Hellenic Geol. Soc., Thessaloniki, Greece, 14–17 April 2004,* 539–540.

Reasenberg, P. A. and Simpson, R. W., 1992. Response of regional seismicity to the static stress change produced by the Loma Prieta earthquake. *Science,* 255, 1687–1690.

Shebalin, N. (editor), 1974. *Catalogue of earthquakes, part III, Atlas of isoseismal maps*, UNDP–UNESCO Survey Seismicity of the Balkan Region, REM/70/172, Skopje.

Tzankov, T. Z., Angelova, D., Nakov, R., Burchfiel, B. C. and Royden, L. H., 1996. The Sub–Balkan graben system of central Bulgaria. *Basin Res.*, 8, 125–142.

Van Eck, R. and Stoyanov, T., 1996. Seismotectonics and seismic hazard modeling for southern Bulgaria. *Tectonophysics*, 262, 310–332.

Vanneste, K., Radulov, A., DeMartini, P., Nikolov, G., Petermans, T., Verbeeck, K., Camelbeeck, T., Pantosti, D., Dimitrov, D. and Shanov, S., 2006. Paleoseismologic investigation of the fault rupture of the 14 April 1928 Chirpan earthquake (M6.8) southern Bulgaria, *J. Geophys. Res.*, 111, B01303, doi:10.1029/2005JB003814.

Wells, D. L. and Coppersmith, K. J., 1994. New empirical relationships among magnitude, rupture length, rupture width, rupture area, and surface displacement. *Bull. Seism. Soc. Am.,* 84, 974–1002.

Wessel, P. and Smith, W. H. F., 1998. New, improved version of the Generic Mapping Tools Released, *EOS Trans. AGU, 79*, 579.

Yankov, Y., 1945. Level changes of the terrain caused by the earthquakes of April 14th and 18th 1928 in south Bulgaria. *Ann. Centr. Mteor. Inst.*, 29–31, 131–136, Sofia.

Zagorchev,I., 1992. Neotectonics of the central parts of the Balkan Peninsula: basic features and concepts. *Geologische Rundshau*, 81, 635–654.